

The layered structure of poly[[hexa-aqua(μ_4 -benzene-1,2,4,5-tetracarboxylato)dicopper(II)] tetrahydrate]

Patricio Cancino,^a Evgenia Spodine,^a Verónica Paredes-García,^b Diego Venegas-Yazigi^c and Andrés Vega^{b*}

^aFacultad de Ciencias Químicas y Farmacéuticas, Universidad de Chile, Sergio Livingstone 1007, Santiago, Chile, ^bDepartamento de Ciencias Químicas, Facultad de Ciencias Exactas, Universidad Andres Bello, Avenida República 275 3er Piso, Santiago, Chile, and ^cFacultad de Química y Biología, Universidad de Santiago de Chile, Casilla 40, Correo 33, Santiago, Chile
Correspondence e-mail: andresvega@unab.cl

Received 6 July 2013

Accepted 26 September 2013

In the structure of the title compound, $\{[\text{Cu}_2(\text{C}_{10}\text{H}_2\text{O}_8)(\text{H}_2\text{O})_6] \cdot 4\text{H}_2\text{O}\}_n$, the benzene-1,2,4,5-tetracarboxylate ligand, $(\text{btec})^{4-}$, is located on a crystallographic inversion centre in a μ_4 -coordination mode. The coordination environment of each pentacoordinated Cu^{II} centre is square pyramidal (SBP), formed by three water molecules and two carboxylate O atoms from two different $(\text{btec})^{4-}$ ligands. The completely deprotonated $(\text{btec})^{4-}$ ligand coordinates in a monodentate mode to four Cu^{II} atoms. The alternation of $(\text{btec})^{4-}$ ligands and SBP Cu^{II} centres leads to the formation of a planar two-dimensional covalent network of parallelograms, parallel to the *ab* plane. Hydrogen bonds between a basal water molecule and an apical one from an adjacent $[\text{Cu}(\text{btec})_{0.5}(\text{H}_2\text{O})_3]$ unit exist in the intralayer space. Hydrogen bonds are also present between the two-dimensional network and the water molecules filling the channels in the structure.

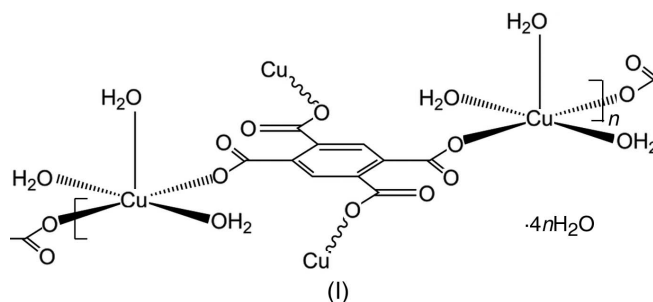
Keywords: crystal structure; metal–organic frameworks (MOFs); benzene-1,2,4,5-tetracarboxylate ligand; Cu complexes.

1. Introduction

Metal–organic frameworks (MOFs) are a family of compounds that are based on metallic ions and polydentate organic ligands, presenting crystalline and porous structures with strong interactions between the metal–ligand entities (Rowsell & Yaghi, 2004). Due to these characteristics, MOFs have been studied extensively in recent years in different fields of chemistry, such as magnetism (Qi *et al.*, 2008), gas storage (Marco-Lozar *et al.*, 2012), luminescent devices (Chen *et al.*, 2007) and catalysis (Nguyen *et al.*, 2012).

The porosity of MOFs depends on the type of organic ligand and the reaction conditions. Different organic ligands,

such as amines, imines, alcohols or carboxylates, have been used, the last being the most common. Carboxylates have a large affinity for divalent and trivalent metal ions, such as Cu^{2+} , Zn^{2+} , Cd^{2+} , In^{3+} , Al^{3+} or Fe^{3+} (Volklinger, Loiseau *et al.*, 2009; Karra *et al.*, 2013; Plaza *et al.*, 2012; Salunke-Gawali *et al.*, 2012).



Benzene-1,2,4,5-tetracarboxylic acid (H_4btec) is a very interesting ligand since it is centrosymmetric and can act in its partial or completely deprotonated forms, thus displaying a variety of coordination modes. The most common anions are the completely deprotonated form, $(\text{btec})^{4-}$, and the doubly deprotonated form, $(\text{H}_2\text{btec})^{2-}$. Thus, the coordination modes of H_4btec can be controlled by regulating the pH, temperature and reaction time. In addition, the synthetic technique used is very important for determining the characteristics of the resulting MOF lattice, the most common techniques being hydrothermal or solvothermal. Hydro(solvo)thermal techniques are very useful, because from a synthetic point of view they represent an easy procedure to obtain new crystalline materials. Using these synthetic methods, the following (btec) complexes have been obtained: $[\text{Cu}(\text{H}_2\text{btec})(\text{bipy})]_n$ (Brown *et al.*, 2009), $[\text{Cu}_2(\text{btec})(\text{bipy})_2]_n$ (*bipy* is 2,2'-bipyridine; Hao *et al.*, 2004), $\{[\text{Cu}(3\text{-tpt})_2(\text{H}_2\text{btec})_2(\text{btec})] \cdot 4\text{H}_2\text{O}\}_n$ [3-tpt is 2,4,6-tris(pyridin-3/4-yl)-1,3,5-triazine; Zhang *et al.*, 2010], $\{[\text{Ni}_2(\text{btec})(\text{bipy})_3] \cdot 3\text{DMF} \cdot 2\text{H}_2\text{O}\}_n$ (DMF is dimethylformamide; Song *et al.*, 2011), $\{[\text{In}_2(\text{OH})_2(\text{H}_2\text{btec})] \cdot 2\text{H}_2\text{O}\}_n$ (Volklinger, Loiseau & Férey, 2009) and $\{[\text{Mg}_{1.5}(\mu_5\text{-btec})(\text{H}_2\text{O})][\text{H}_2\text{N}(\text{CH}_3)_2]\}_n$ (Zhang *et al.*, 2007).

Other synthetic procedures which have been reported in the literature to produce crystalline *btec*-based MOFs are the ionothermal and microwave-assisted techniques. The former uses an ionic liquid as the reaction medium, leading to complexes like $\{[\text{K}_2(\text{H}_2\text{O})_6][\text{Cd}_3(\text{btec})_2]\}_n$ (Ji *et al.*, 2008), while microwave-assisted synthesis produced $[\text{Zn}_4\text{O}(\text{BDC})_3 \cdot \text{H}_2\text{O}]$ (IRMOF-1) in only 25 s (BDC is benzene-1,4-dicarboxylate; Ni & Masel, 2006).

A two-dimensional polymeric Cu^{II} complex without auxiliary ligands, $[\text{Cu}(\text{btec})_{0.5}(\text{DMF})]_n$, was obtained in a non-aqueous medium by simply stirring a methanolic solution of a Cu^{II} salt with a DMF solution of H_4btec (Zhao *et al.*, 2007).

We report herein a new Cu^{II} metal–organic framework based on completely deprotonated benzene-1,2,4,5-tetracarboxylic acid, *viz.* $\{[\text{Cu}_2(\text{btec})(\text{H}_2\text{O})_6] \cdot 4\text{H}_2\text{O}\}_n$ (I), without the presence of auxiliary ligands and obtained under reflux in an aqueous medium.

Table 1

Experimental details.

Crystal data	
Chemical formula	[Cu ₂ (C ₁₀ H ₂ O ₈)(H ₂ O) ₆].4H ₂ O
<i>M_r</i>	278.68
Crystal system, space group	Monoclinic, <i>C2/c</i>
Temperature (K)	296
<i>a</i> , <i>b</i> , <i>c</i> (Å)	12.1571 (3), 18.1138 (4), 9.6370 (4)
β (°)	113.405 (1)
<i>V</i> (Å ³)	1947.56 (10)
<i>Z</i>	8
Radiation type	Mo <i>K</i> α
μ (mm ⁻¹)	2.27
Crystal size (mm)	0.75 × 0.42 × 0.36
Data collection	
Diffractometer	Bruker SMART APEXII area-detector diffractometer
Absorption correction	Empirical (using intensity measurements) (<i>SADABS</i> ; Bruker, 2001)
<i>T_{min}</i> , <i>T_{max}</i>	0.281, 0.493
No. of measured, independent and observed [<i>I</i> > 2 σ (<i>I</i>)] reflections	4973, 1911, 1773
<i>R_{int}</i>	0.000
(<i>sin</i> θ / λ) _{max} (Å ⁻¹)	0.617
Refinement	
<i>R</i> [<i>F</i> ² > 2 σ (<i>F</i> ²)], <i>wR</i> (<i>F</i> ²), <i>S</i>	0.029, 0.083, 1.08
No. of reflections	1911
No. of parameters	142
No. of restraints	6
H-atom treatment	H atoms treated by a mixture of independent and constrained refinement
$\Delta\rho_{max}$, $\Delta\rho_{min}$ (e Å ⁻³)	0.92, -0.48

Computer programs: *APEX2* (Bruker, 2001), *SAINT* (Bruker, 2001), *SHELXS97* (Sheldrick, 2008), *SHELXL97* (Sheldrick, 2008) and *SHELXTL* (Bruker, 2001).

2. Experimental

2.1. Synthesis and crystallization

Benzene-1,2,4,5-tetracarboxylic acid (H₄btec; 96%, Aldrich), CuO (99%, Aldrich) and Gd₂O₃ (99%, Merck) were used as received. A mixture of solid CuO (0.039 g, 0.49 mmol), Gd₂O₃ (0.051 g, 0.14 mmol), H₄btec (0.271 g, 1.07 mmol) and deionized water (250 ml) was placed in a flask connected to a condenser. The mixture was stirred for 8 h under reflux, and then the reaction was left to cool to room temperature. The resulting solution was filtered, concentrated and left for crystallization at 277 K for two months. Blue crystals of (I) were formed, and these were washed with cold water and dried at room temperature. Analysis calculated for C₂₀H₁₀CuO₁₉: Cu 10.29, C 38.90, H 1.62%; found: Cu 10.67, C 39.15, H 1.73%. The FT-IR spectrum of (I) in KBr pellets presented the following bands: H₂O (OH) 3390 cm⁻¹; monodentate carboxylate 1591 (asym) and 1386 cm⁻¹ (sym).

2.2. Refinement

Crystal data, data collection and structure refinement details are summarized in Table 1. The aromatic H-atom position was calculated after each cycle of refinement using a riding model, with C–H = 0.93 Å and *U*_{iso}(H) = 1.2*U*_{eq}(parent). Aqua H atoms were located in the final difference Fourier map and subsequently refined isotropically with O–H distances restrained tightly to 0.870 (1) Å. During the structure completion process, it became clear that residual

electron density was present in the channels formed by the covalent copper(II)/(btec)⁴⁻ network. Preliminary analysis suggested that it corresponded to uncoordinated solvent water molecules. Efforts to model the density as water molecules with their respective H atoms gave no fully satisfactory results, and so the remaining electron density was modelled using SQUEEZE in *PLATON* (Spek, 2009). This leads to about 120 e⁻ for the unit cell. Although the amount of solvating water corresponds to one and a half water molecules per asymmetric unit, previous refinement/Fourier difference map work clearly suggested this number would be two; there was no meaningful remaining unassigned electron density and the O atoms had normal displacement parameters. Thus, we retained this amount (two solvent water molecules) for the formula and the structural report.

3. Results and discussion

The unique feature of the title polymeric complex, {[Cu₂(btec)(H₂O)₆].4H₂O}_{*n*}, (I), is that the completely deprotonated ligand coordinates to four metal atoms in monodentate modes, while in the above-mentioned polymer, [Cu(btec)_{0.5}(DMF)]_{*n*} (Zhao *et al.*, 2007), the same (btec)⁴⁻ ligand is bidentate and binds the metal centres into a typical paddle-wheel-like building block.

The structure of (I) is constructed out of alternating pentacoordinated Cu^{II} centres and (btec)⁴⁻ ligands. The centroid of the (btec)⁴⁻ anion lies on a crystallographic inversion centre and therefore the fragment has *C_i* symmetry. The anion is connected to four equivalent Cu^{II} centres, displaying a μ_4 -coordination mode. The coordination environment around the metal centre is formed by three water molecules and two carboxylate O atoms from two (btec)⁴⁻ anions (Fig. 1 and Table 2). The coordination geometry is best described as a square-based pyramid (SBP) (τ = 0.02; Addison *et al.*, 1984), having two water molecules and two carboxylate O atoms in the basal plane, in a *trans* disposition, and a water molecule at the apical position. Interestingly, the Cu^{II} centre shows almost

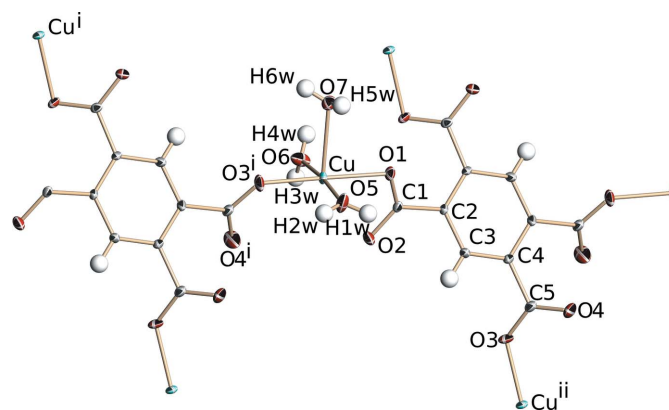


Figure 1 Part of the structure of (I), showing the coordination around the Cu^{II} centre and the atom-numbering scheme. Displacement ellipsoids are drawn at the 50% probability level. [Symmetry codes: (i) $-x + \frac{1}{2}, y - \frac{1}{2}, -z + \frac{3}{2}$; (ii) $-x + \frac{1}{2}, y + \frac{1}{2}, -z + \frac{3}{2}$.]

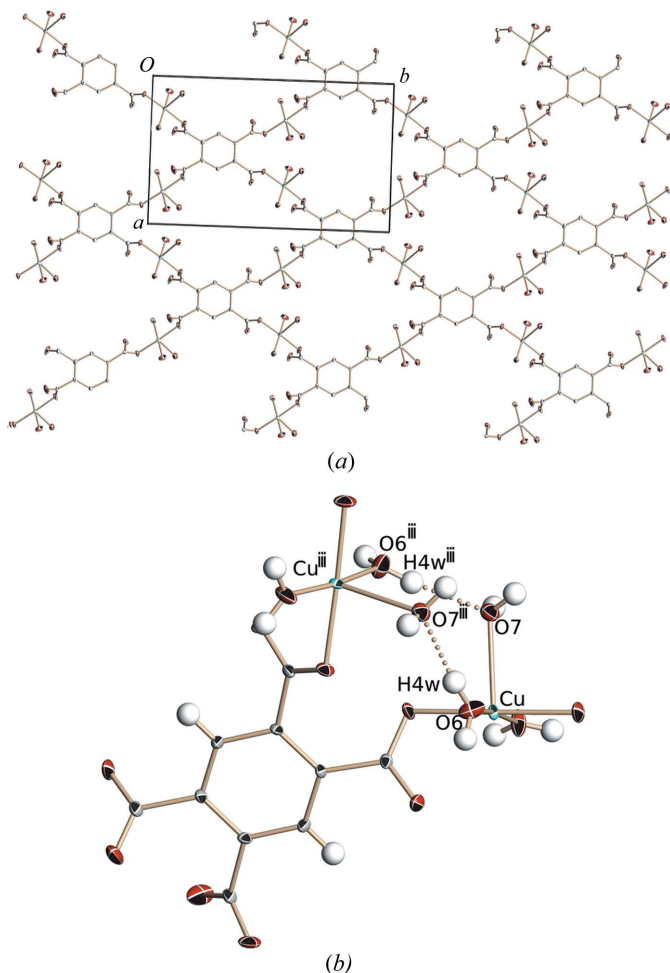


Figure 2
 (a) A packing view for (I), along [001], showing the covalent layers along the *ab* plane. (b) Detail showing the intralayer hydrogen bonds (dotted lines) between apical and equatorial water molecules on neighbouring Cu^{II} centres. [Symmetry code: (iii) $-x + 1, y, -z + \frac{3}{2}$.]

no deviation towards the apical position (0.03 Å). The ligand is considered to have a monodentate coordination mode because of the considerably longer distances from Cu^{II} to the uncoordinated carboxylate O atoms O2 [2.6748 (18) Å] and O4ⁱ [3.221 (3) Å; symmetry code: (i) $-x + \frac{1}{2}, y - \frac{1}{2}, -z + \frac{3}{2}$]. The

Table 2
 Selected geometric parameters (Å, °).

Cu1—O6	1.949 (2)	Cu1—O1	2.0087 (17)
Cu1—O3 ⁱ	1.9513 (18)	Cu1—O7	2.248 (2)
Cu1—O5	1.956 (2)		
O6—Cu—O3 ⁱ	91.34 (9)	O5—Cu—O1	88.74 (8)
O6—Cu—O5	173.67 (9)	O6—Cu—O7	91.10 (8)
O3 ⁱ —Cu—O5	86.44 (8)	O3 ⁱ —Cu—O7	92.88 (8)
O6—Cu—O1	93.56 (9)	O5—Cu—O7	94.93 (8)
O3 ⁱ —Cu—O1	175.08 (8)	O1—Cu—O7	86.52 (7)

Symmetry codes: (i) $-x + \frac{1}{2}, y - \frac{1}{2}, -z + \frac{3}{2}$.

Table 3
 Hydrogen-bond geometry (Å, °).

<i>D</i> —H... <i>A</i>	<i>D</i> —H	H... <i>A</i>	<i>D</i> ... <i>A</i>	<i>D</i> —H... <i>A</i>
O6—H4W...O7 ⁱⁱⁱ	0.87	1.84	2.698 (3)	170
O5—H1W...O4 ^{iv}	0.87	1.85	2.679 (3)	160
O7—H5W...O2 ^v	0.87	1.90	2.679 (3)	148
O6—H3W...O1 ^{vi}	0.87	2.00	2.826 (3)	157

Symmetry codes: (iii) $-x + 1, y, -z + \frac{3}{2}$; (iv) $-x + \frac{1}{2}, -y + \frac{3}{2}, -z + 1$; (v) $x, -y + 1, z - \frac{1}{2}$; (vi) $x, -y + 1, z + \frac{1}{2}$.

carboxylate groups are not coplanar with the basal coordination plane of the pyramid and form dihedral angles of 75.81 (6) and 65.59 (6)° with its least-squares plane.

The tetra-monodentate μ_4 -coordination mode displayed by the (btec)⁴⁻ anion, in addition to the SBP and the *trans* coordination mode around each Cu^{II} centre, leads to the formation of a planar two-dimensional covalent network parallel to the *ab* plane (Fig. 2a). The network can be considered as formed by regular parallelograms with a side of 10.908 (4) Å [Cu1...Cu1($x + \frac{1}{2}, y + \frac{1}{2}, z$)]. Intralayer hydrogen bonds between a basal water molecule and an apical water molecule from an adjacent metal centre (and *vice versa*) (O6...O7ⁱⁱⁱ; see Table 3 for full details) contribute to the stabilization of the two-dimensional lattice (Fig. 2b).

The rigid nature of the (btec)⁴⁻ anion, coordinated to the Cu^{II} centres, leads to the presence of a large elliptical space inside each parallelogram (Fig. 2a). The above-mentioned inclination of the basal plane of the coordination pyramid around the Cu^{II} centre in relation to the carboxylate groups leads to two important consequences: (a) the two basal *trans*

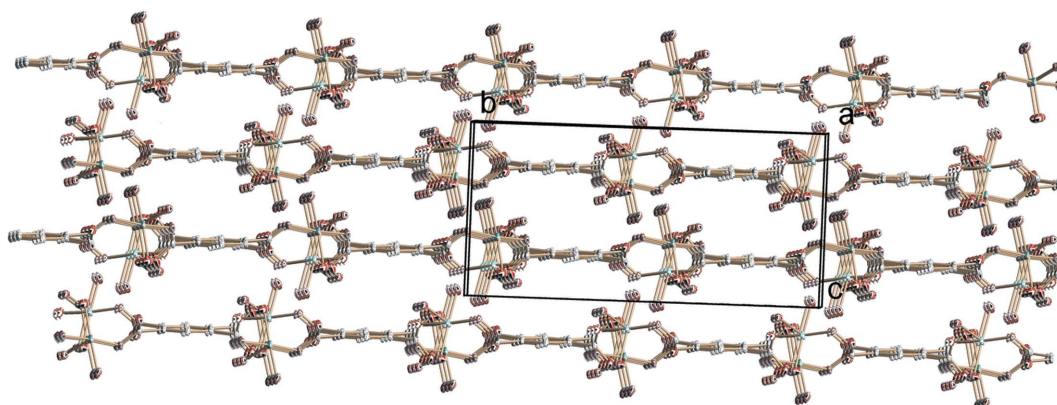


Figure 3
 A packing view for (I), along [100], showing consecutive two-dimensional layers and the presence of channels in this direction.

water molecules point to opposite sides of the two-dimensional covalent network and (b) the apical water molecule points directly to the elliptical space.

As shown in Fig. 3, two consecutive two-dimensional layers are separated by 9.6370 (4) Å (*c* cell axis). No covalent interactions are found between them, but several strong hydrogen bonds exist, as shown in Table 3. The relative position of the layers leads to the formation of channels along the [100] direction (Fig. 3). These channels are assumed to be filled by solvent water molecules (omitted from the model by the SQUEEZE procedure as described in §2.2), which are also presumably hydrogen bonded to the covalent coordination network layers.

The authors acknowledge financial support from Beca CONICYT 21110228 'Programa de Formación de Capital Humano Avanzado' and Financiamiento Basal para Centros Científicos y Tecnológicos de Excelencia (grant No. FB0807).

Supplementary data for this paper are available from the IUCr electronic archives (Reference: YF3042). Services for accessing these data are described at the back of the journal.

References

- Addison, A. W., Rao, T. N., Reedijk, J., Van Rijn, J. & Verschoor, G. C. (1984). *J. Chem. Soc. Dalton Trans.* pp. 1349–1356.
- Brown, K., Zolezzi, S., Aguirre, P., Venegas-Yazigi, D., Paredes-García, V., Baggio, R., Novak, M. A. & Spodine, E. (2009). *Dalton Trans.* pp. 1422–1427.
- Bruker (2001). *APEX2* and *SADABS*. Bruker AXS Inc., Madison, Wisconsin, USA.
- Chen, B., Yang, Y., Zapata, F., Lin, G., Qian, G. & Lobkovsky, E. B. (2007). *Adv. Mater.* **19**, 1693–1696.
- Hao, N., Li, Y., Wang, E., Sheng, E., Hu, C. & Xu, L. (2004). *J. Mol. Struct.* **697**, 1–8.
- Ji, W., Zhai, Q., Hu, M., Li, S., Jiang, Y. & Wang, Y. (2008). *Inorg. Chem. Commun.* **11**, 1455–1458.
- Karra, J. R., Grabicka, B. E., Huang, Y. & Walton, K. S. (2013). *J. Colloid Interface Sci.* **392**, 331–336.
- Marco-Lozar, J. P., Juan-Juan, J., Suarez-Garcia, F., Cazorla-Amoros, D. & Linares-Solano, A. (2012). *Int. J. Hydrogen Energy*, **37**, 2370–2381.
- Nguyen, L. T. L., Nguyen, T. T., Nguyen, K. & Phan, D. N. T. S. (2012). *Appl. Catal. A*, **426**, 44–52.
- Ni, Z. & Masel, R. L. (2006). *J. Am. Chem. Soc.* **128**, 12394–12395.
- Plaza, M. G., Ribeiro, A. M., Ferreira, A., Santos, J. C., Hwang, Y. K., Seo, Y. K., Lee, U. H., Chang, J. S., Loureiro, J. M. & Rodrigues, A. E. (2012). *Microporous Mesoporous Mater.* **153**, 178–190.
- Qi, C., Zhang, D., Gao, S., Ma, H., He, Y., Ma, S., Chen, Y. & Yang, X. (2008). *J. Mol. Struct.* **891**, 357–363.
- Rowell, J. L. C. & Yaghi, O. M. (2004). *Microporous Mesoporous Mater.* **73**, 3–14.
- Salunke-Gawali, S., Kathawate, L. & Puranik, V. G. (2012). *J. Mol. Struct.* **1022**, 189–196.
- Sheldrick, G. M. (2008). *Acta Cryst.* **A64**, 112–122.
- Song, P., Li, Y., He, B., Yang, J., Zheng, J. & Li, X. (2011). *Microporous Mesoporous Mater.* **142**, 208–213.
- Spek, A. L. (2009). *Acta Cryst.* **D65**, 148–155.
- Volklinger, C., Loiseau, T. & Férey, G. (2009). *Solid State Sci.* **11**, 29–35.
- Volklinger, C., Loiseau, T., Guillou, N., Férey, G., Haouas, M., Taulelle, F., Audebrand, N., Margiolaki, I., Popov, D., Burghammer, M. & Riekel, C. (2009). *Cryst. Growth Des.* **9**, 2927–2936.
- Zhang, N., Li, M., Wang, Z., Shao, M. & Zhu, S. (2010). *Inorg. Chim. Acta*, **363**, 8–14.
- Zhang, D., Song, T., Zhang, P., Shi, J., Wang, Y., Wang, L., Ma, K., Yin, W., Zhao, J., Fan, Y. & Xu, J. (2007). *Inorg. Chem. Commun.* **10**, 876–879.
- Zhao, H., Ding, B., Yang, E., Wang, X. & Zhao, X. (2007). *Z. Anorg. Allg. Chem.* **633**, 1735–1738.

supplementary materials

Acta Cryst. (2013). C69, 1344-1347 [doi:10.1107/S0108270113026620]

The layered structure of poly[[hexaaqua(μ_4 -benzene-1,2,4,5-tetracarboxylato)dicopper(II)] tetrahydrate]

Patricio Cancino, Evgenia Spodine, Verónica Paredes-García, Diego Venegas-Yazigi and Andrés Vega

Computing details

Data collection: *APEX2* (Bruker, 2001); cell refinement: *SAINTE* (Bruker, 2001); data reduction: *SAINTE* (Bruker, 2001); program(s) used to solve structure: *SHELXS97* (Sheldrick, 2008); program(s) used to refine structure: *SHELXL97* (Sheldrick, 2008); molecular graphics: *SHELXTL* (Bruker, 2001); software used to prepare material for publication: *SHELXTL* (Bruker, 2001).

Poly[[hexaaqua(μ_4 -benzene-1,2,4,5-tetracarboxylato)dicopper(II)] tetrahydrate]

Crystal data

$[\text{Cu}_2(\text{C}_{10}\text{H}_2\text{O}_8)(\text{H}_2\text{O})_6] \cdot 4\text{H}_2\text{O}$

$M_r = 278.68$

Monoclinic, *C2/c*

Hall symbol: -C 2yc

$a = 12.1571$ (3) Å

$b = 18.1138$ (4) Å

$c = 9.6370$ (4) Å

$\beta = 113.405$ (1)°

$V = 1947.56$ (10) Å³

$Z = 8$

$F(000) = 1136$

$D_x = 1.901$ Mg m⁻³

Mo $K\alpha$ radiation, $\lambda = 0.71073$ Å

Cell parameters from 5027 reflections

$\theta = 3.2\text{--}26.1^\circ$

$\mu = 2.27$ mm⁻¹

$T = 296$ K

Needle, blue

$0.75 \times 0.42 \times 0.36$ mm

Data collection

Bruker SMART APEXII area-detector diffractometer

Radiation source: fine-focus sealed tube

Graphite monochromator

φ and ω scans

Absorption correction: empirical (using intensity measurements)

(*SADABS*; Bruker, 2001)

$T_{\min} = 0.281$, $T_{\max} = 0.493$

4973 measured reflections

1911 independent reflections

1773 reflections with $I > 2\sigma(I)$

$R_{\text{int}} = 0.0000$

$\theta_{\max} = 26.0^\circ$, $\theta_{\min} = 2.6^\circ$

$h = -14 \rightarrow 14$

$k = 0 \rightarrow 22$

$l = 0 \rightarrow 11$

Refinement

Refinement on F^2

Least-squares matrix: full

$R[F^2 > 2\sigma(F^2)] = 0.029$

$wR(F^2) = 0.083$

$S = 1.08$

1911 reflections

142 parameters

6 restraints

Primary atom site location: structure-invariant

direct methods

Secondary atom site location: difference Fourier

map

Hydrogen site location: inferred from
neighbouring sites
H atoms treated by a mixture of independent
and constrained refinement

$$w = 1/[\sigma^2(F_o^2) + (0.0333P)^2 + 2.2354P]$$

where $P = (F_o^2 + 2F_c^2)/3$
 $(\Delta/\sigma)_{\max} = 0.001$
 $\Delta\rho_{\max} = 0.92 \text{ e } \text{\AA}^{-3}$
 $\Delta\rho_{\min} = -0.48 \text{ e } \text{\AA}^{-3}$

Special details

Geometry. All e.s.d.'s (except the e.s.d. in the dihedral angle between two l.s. planes) are estimated using the full covariance matrix. The cell e.s.d.'s are taken into account individually in the estimation of e.s.d.'s in distances, angles and torsion angles; correlations between e.s.d.'s in cell parameters are only used when they are defined by crystal symmetry. An approximate (isotropic) treatment of cell e.s.d.'s is used for estimating e.s.d.'s involving l.s. planes.

Least-squares planes (x,y,z in crystal coordinates) and deviations from them (* indicates atom used to define plane)
 $-8.2615 (0.0049) x + 11.0944 (0.0074) y + 6.1727 (0.0045) z = 6.7576 (0.0042)$

* $-0.0345 (0.0006) \text{ Cu} * -0.0458 (0.0007) \text{ O1} * 0.0630 (0.0008) \text{ O6} * 0.0670 (0.0008) \text{ O5} * -0.0497 (0.0008) \text{ O3_}\8

Rms deviation of fitted atoms = 0.0533

$5.5927 (0.0102) x - 7.4133 (0.0147) y + 5.2077 (0.0074) z = 1.5270 (0.0108)$

Angle to previous plane (with approximate e.s.d.) = 75.81 (0.06)

* $-0.0041 (0.0005) \text{ O1} * 0.0115 (0.0014) \text{ C1} * -0.0033 (0.0004) \text{ C2} * -0.0041 (0.0005) \text{ O2}$

Rms deviation of fitted atoms = 0.0066 the $7.3951 (0.0096) x - 7.9113 (0.0178) y + 3.5326 (0.0095) z = 0.8877 (0.0105)$

Angle to previous plane (with approximate e.s.d.) = 65.59 (0.06)

* $0.0021 (0.0006) \text{ O3_}\$8 * -0.0058 (0.0016) \text{ C5_}\$8 * 0.0016 (0.0004) \text{ C4_}\$8 * 0.0022 (0.0006) \text{ O4_}\8

Rms deviation of fitted atoms = 0.0034

Refinement. Refinement of F^2 against ALL reflections. The weighted R -factor wR and goodness of fit S are based on F^2 , conventional R -factors R are based on F , with F set to zero for negative F^2 . The threshold expression of $F^2 > \sigma(F^2)$ is used only for calculating R -factors(gt) *etc.* and is not relevant to the choice of reflections for refinement. R -factors based on F^2 are statistically about twice as large as those based on F , and R -factors based on ALL data will be even larger.

Fractional atomic coordinates and isotropic or equivalent isotropic displacement parameters (\AA^2)

	x	y	z	$U_{\text{iso}}^*/U_{\text{eq}}$
Cu1	0.27996 (2)	0.441393 (15)	0.67052 (3)	0.01200 (13)
O1	0.37365 (16)	0.52682 (9)	0.64069 (19)	0.0148 (4)
C1	0.3665 (2)	0.57872 (13)	0.7256 (3)	0.0111 (5)
O2	0.29745 (17)	0.57583 (10)	0.7923 (2)	0.0195 (4)
C2	0.4398 (2)	0.64728 (13)	0.7414 (3)	0.0102 (5)
C3	0.3825 (2)	0.71442 (13)	0.7360 (3)	0.0132 (5)
H5A	0.3036	0.7145	0.7276	0.016*
C4	0.4407 (2)	0.78137 (13)	0.7429 (3)	0.0125 (5)
C5	0.3723 (2)	0.85229 (13)	0.7288 (3)	0.0148 (5)
O3	0.32031 (17)	0.85931 (10)	0.8187 (2)	0.0207 (4)
O4	0.3696 (2)	0.89728 (12)	0.6308 (3)	0.0337 (5)
O5	0.15185 (18)	0.46427 (11)	0.4747 (2)	0.0250 (4)
H1W	0.157 (4)	0.5056 (15)	0.431 (5)	0.073 (15)*
H2W	0.082 (2)	0.445 (3)	0.454 (6)	0.082 (19)*
O6	0.39550 (18)	0.42212 (13)	0.8757 (2)	0.0251 (4)
H3W	0.392 (5)	0.450 (2)	0.948 (4)	0.076 (17)*
H4W	0.4656 (19)	0.402 (2)	0.900 (5)	0.062 (14)*
O7	0.38393 (17)	0.37018 (11)	0.5742 (2)	0.0201 (4)
H5W	0.346 (4)	0.370 (3)	0.4764 (7)	0.080 (17)*
H6W	0.383 (3)	0.3226 (3)	0.586 (4)	0.031 (9)*

Atomic displacement parameters (\AA^2)

	U^{11}	U^{22}	U^{33}	U^{12}	U^{13}	U^{23}
Cu1	0.01281 (19)	0.00741 (18)	0.01753 (19)	-0.00314 (10)	0.00786 (13)	0.00076 (10)
O1	0.0199 (9)	0.0082 (8)	0.0188 (9)	-0.0044 (7)	0.0103 (7)	-0.0026 (7)
C1	0.0095 (11)	0.0085 (11)	0.0146 (11)	0.0005 (9)	0.0041 (9)	0.0022 (9)
O2	0.0205 (9)	0.0157 (9)	0.0294 (10)	-0.0050 (7)	0.0175 (8)	-0.0030 (8)
C2	0.0122 (11)	0.0058 (11)	0.0142 (11)	-0.0008 (9)	0.0069 (9)	-0.0001 (8)
C3	0.0109 (10)	0.0093 (12)	0.0211 (12)	0.0007 (9)	0.0083 (10)	0.0021 (9)
C4	0.0155 (12)	0.0077 (11)	0.0183 (11)	0.0019 (9)	0.0110 (10)	0.0008 (9)
C5	0.0142 (11)	0.0072 (11)	0.0237 (12)	0.0000 (9)	0.0081 (10)	-0.0006 (9)
O3	0.0261 (10)	0.0142 (9)	0.0281 (10)	0.0096 (8)	0.0174 (8)	0.0020 (8)
O4	0.0447 (13)	0.0188 (11)	0.0524 (14)	0.0142 (9)	0.0350 (12)	0.0191 (10)
O5	0.0183 (10)	0.0176 (10)	0.0314 (11)	-0.0040 (8)	0.0019 (8)	0.0087 (9)
O6	0.0225 (10)	0.0347 (12)	0.0196 (10)	0.0081 (9)	0.0100 (8)	0.0022 (9)
O7	0.0232 (10)	0.0158 (10)	0.0233 (10)	0.0000 (8)	0.0113 (8)	-0.0013 (8)

Geometric parameters (\AA , $^\circ$)

Cu1—O6	1.949 (2)	C3—C4	1.392 (3)
Cu1—O3 ⁱ	1.9513 (18)	C3—H5A	0.9300
Cu1—O5	1.956 (2)	C4—C4 ⁱⁱⁱ	1.393 (5)
Cu1—O1	2.0087 (17)	C4—C5	1.507 (3)
Cu1—O7	2.248 (2)	C5—O4	1.238 (3)
O3—Cu1 ⁱⁱ	1.9513 (18)	C5—O3	1.266 (3)
Cu1—Cu1 ⁱ	9.2625 (5)	O5—H1W	0.8700
O1—C1	1.272 (3)	O5—H2W	0.8700
C1—O2	1.244 (3)	O6—H3W	0.8700
C1—C2	1.501 (3)	O6—H4W	0.8700
C2—C3	1.392 (3)	O7—H5W	0.8700
C2—C2 ⁱⁱⁱ	1.406 (5)	O7—H6W	0.8700
O6—Cu1—O3 ⁱ	91.34 (9)	C2—C3—H5A	119.3
O6—Cu1—O5	173.67 (9)	C4—C3—H5A	119.3
O3 ⁱ —Cu1—O5	86.44 (8)	C3—C4—C4 ⁱⁱⁱ	119.42 (14)
O6—Cu1—O1	93.56 (9)	C3—C4—C5	119.1 (2)
O3 ⁱ —Cu1—O1	175.08 (8)	C4 ⁱⁱⁱ —C4—C5	121.43 (13)
O5—Cu1—O1	88.74 (8)	O4—C5—O3	126.0 (2)
O6—Cu1—O7	91.10 (8)	O4—C5—C4	118.4 (2)
O3 ⁱ —Cu1—O7	92.88 (8)	O3—C5—C4	115.5 (2)
O5—Cu1—O7	94.93 (8)	C5—O3—Cu1 ⁱⁱ	127.24 (17)
O1—Cu1—O7	86.52 (7)	Cu1—O5—H1W	118
C1—O1—Cu1	106.82 (15)	Cu1—O5—H2W	118
O2—C1—O1	122.3 (2)	H1W—O5—H2W	119
O2—C1—C2	118.6 (2)	Cu1—O6—H3W	118
O1—C1—C2	119.1 (2)	Cu1—O6—H4W	125
C3—C2—C2 ⁱⁱⁱ	119.11 (14)	H3W—O6—H4W	112
C3—C2—C1	116.8 (2)	Cu1—O7—H5W	108
C2 ⁱⁱⁱ —C2—C1	124.10 (13)	Cu1—O7—H6W	118
C2—C3—C4	121.4 (2)	H5W—O7—H6W	97

O6—Cu1—O1—C1	-69.63 (16)	C2 ⁱⁱⁱ —C2—C3—C4	1.9 (4)
O3 ⁱ —Cu1—O1—C1	116.5 (9)	C1—C2—C3—C4	-177.2 (2)
O5—Cu1—O1—C1	104.47 (16)	C2—C3—C4—C4 ⁱⁱⁱ	-0.6 (4)
O7—Cu1—O1—C1	-160.52 (16)	C2—C3—C4—C5	176.9 (2)
Cu1—O1—C1—O2	-9.6 (3)	C3—C4—C5—O4	-125.5 (3)
Cu1—O1—C1—C2	173.00 (16)	C4 ⁱⁱⁱ —C4—C5—O4	52.0 (4)
O2—C1—C2—C3	-41.2 (3)	C3—C4—C5—O3	53.2 (3)
O1—C1—C2—C3	136.3 (2)	C4 ⁱⁱⁱ —C4—C5—O3	-129.2 (3)
O2—C1—C2—C2 ⁱⁱⁱ	139.7 (3)	O4—C5—O3—Cu1 ⁱⁱ	0.7 (4)
O1—C1—C2—C2 ⁱⁱⁱ	-42.8 (4)	C4—C5—O3—Cu1 ⁱⁱ	-177.94 (16)

Symmetry codes: (i) $-x+1/2, y-1/2, -z+3/2$; (ii) $-x+1/2, y+1/2, -z+3/2$; (iii) $-x+1, y, -z+3/2$.

Hydrogen-bond geometry (Å, °)

<i>D—H...A</i>	<i>D—H</i>	<i>H...A</i>	<i>D...A</i>	<i>D—H...A</i>
O6—H4W...O7 ⁱⁱⁱ	0.87	1.84	2.698 (3)	170
O5—H1W...O4 ^{iv}	0.87	1.85	2.679 (3)	160
O7—H5W...O2 ^v	0.87	1.90	2.679 (3)	148
O6—H3W...O1 ^{vi}	0.87	2.00	2.826 (3)	157

Symmetry codes: (iii) $-x+1, y, -z+3/2$; (iv) $-x+1/2, -y+3/2, -z+1$; (v) $x, -y+1, z-1/2$; (vi) $x, -y+1, z+1/2$.